Directional Multipath Exploitation for Stationary Target Localization with a Single-Antenna

A. H. Muqaibel
Electrical Engineering Department
King Fahd University of Petroleum & Minerals
P.O. Box 1734, Dhahran 31261, Saudi Arabia

M. G. Amin, F. Ahmad
Center for Advanced Communications
Villanova University
Villanova, PA 19085, USA

***Abstract*— In this paper, we propose a new multipath exploitation approach for stationary urban target localization with a single radar unit. The proposed non-coherent approach utilizes the embedded directivity in ultra wideband (UWB) antennas to estimate target positions using interior wall multipath returns. We assume resolvability of the multipath components, which is made possible by virtue of using UWB radar signals. This approach is most attractive when only few multipaths are detectable due to propagation obstructions or owing to their corresponding low signal-to-noise ratios. Supporting simulations results are provided.**

I. INTRODUCTION

Multipath propagation arises in urban and through-the-wall radar sensing due to electromagnetic (EM) interactions of targets of interest with surrounding objects and surfaces. This leads to highly cluttered images, thereby compromising image quality and interpretation.

Multipath exploitation approaches have been employed recently in indoor target localization [1]-[5]. The goal of such approaches is not to suppress multipath returns, but rather use their energy to aid in the localization process. Multipath exploitation, however, requires prior knowledge of the location of major scatterers in the radar field of view. For targets inside enclosed structures, this implies requiring information on interior building layouts, which, if not available in the form of blueprints, can be determined from prior surveillance operations.

When viewed by an imaging system using physical or synthesized aperture, target multipath returns cause ghosts, which were folded in [1, 6] to the target image, leading to enhanced image and increased signal to clutter ratio. Further, shadowed regions of spatially extended targets were revealed via their multipath returns in [7], whereas an inverse scattering based multipath exploitation approach was presented in [5] for imaging stationary targets in urban canyons with enhanced cross-range resolution. Multipath exploitation methods for target classification and sparse reconstruction in through-the-wall radar imaging applications were examined in [8, 9], respectively.

The work by A. H. Muqaibel was supported by the Deanship of Scientific Research at King Fahd University of Petroleum & Minerals (KFUPM).

In this paper, we consider multipath exploitation for sensing indoor stationary scenes using a single-antenna ultra wideband (UWB) radar system. Deploying a physical or synthesized array aperture could be costly and logistically difficult compared to a less expensive and more flexible single-antenna radar system. In this case, one has to exploit multipath returns resulting from the EM interactions between targets and surrounding walls to enable cross-range estimations. The concept of exploitation is embedded in using the resolvable multipath to create virtual radar units at different locations dictated by the positions of both targets and walls. Incoherent localizations can then proceed using constant-range contours corresponding to monostatic and bistatic two-way propagation between the actual radar unit, the targets, and the virtual radar units.

While the above single-antenna radar system based multipath exploitation concept was already discussed in our earlier work [4], this paper offers a fundamentally different and more effective approach for target localization. The proposed new approach uses an important property of UWB antennas which has been ignored in the underlying application thus far. That is, the received waveform varies as a function of the signal's direction of arrival (DOA), as illustrated in Fig. 1. This figure depicts the received signals from a flat metal plate measured with a UWB ridged horn antenna for six different angular antenna orientations, with 90° representing normal incidence. This property lends itself to reducing the number of required multipath returns. This is achieved by discarding false solutions whose corresponding pulse shapes deviate from that of the received pulse. Only one single bounce multipath component from a side or a back wall in addition to the direct return, are required for target localization. This enables forming a circle and an ellipse with known center and foci, respectively. With only two returns required for target localization, and in absence of Doppler measurements and information, we relax the requirements of the previously published wall association algorithm in [4], which assumes the resolvability of all single bounce and double bounce multipath components.

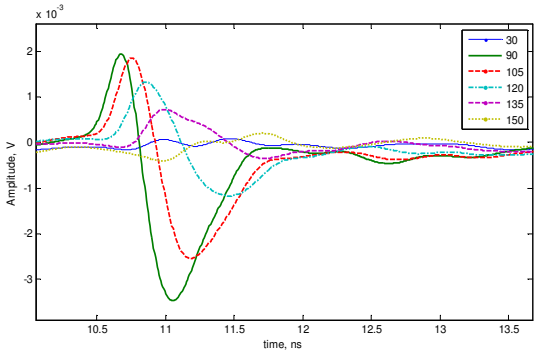

Fig. 1. Variation of the received signal with the antenna angle for horizontal polarization.

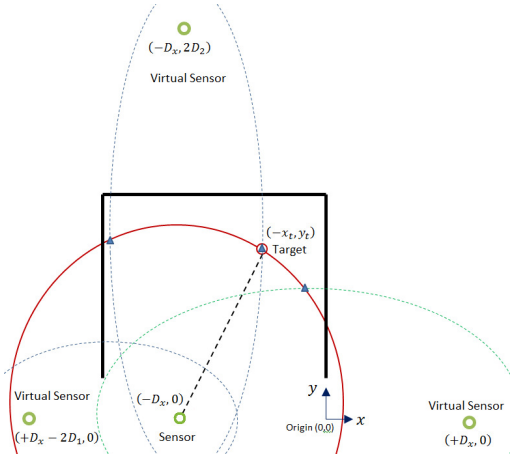

Fig. 2. Multipath model and scene geometry.

The paper is organized as follows. Section II presents the multipath model and the proposed localization scheme based on two resolvable arrivals. Section III provides supporting simulation results. Sensitivity of the proposed scheme to errors in time-of-arrival estimates is discussed in Section IV. Section V provides the concluding remarks.

II. Proposed Localization Scheme

The problem geometry is depicted in Fig. 2. The target is located at position $(-x_t, y_t)$ within three walls. Note that the model can be readily extended to the case where the targets are located inside enclosed structures. The right side wall is located at $x = 0$. The side walls have a length of D_2 meters, whereas the back wall has an extent of D_1 meters. The sensor is located at $(-D_x,0)$m. The azimuth angle is measured from the x-axis. To keep the problem in two dimensions, the elevation angle is fixed at 0° measured from the $x-y$ plane.

We consider a total of four possible paths by which the signal can travel from the sensor to the target and back. The first is the direct path, which does not involve any secondary reflection at an interior wall. Three single-bounce multipath components involving a reflection at an interior wall either on transit to or back from the target are assumed. Higher order multipath components are not utilized for localization and are, therefore, ignored in this paper.

The walls are assumed to be perfect reflectors. When the radar transmits a pulsed signal, $s(t)$, the received signal, $r(t)$, is a superposition of the direct path and the multipath returns, and can be expressed as:

$$r(t) = \sum_{i=1}^{N} A_i s_i(t - \tau_i) + n(t) \tag{1}$$

where N is the total number of signal components, and A_i and τ_i are the amplitude and delay of the ith component, respectively. The ith signal component is denoted by $s_i(\cdot)$, suggesting that the returns are not just delayed and scaled version of the transmit pulse but can also assume different shapes. We assume that the components of the radar return in (1) are resolvable. The times-of-arrival (TOA) for the first two arrivals, τ_1 and τ_2, with the first one corresponding to the direct path and the second to a single bounce multipath, are readily available.

From the underlying monostatic configuration, the target location according to the first arrival is confined to the constant range contour given by

$$(x + D_x)^2 + y^2 - \frac{\tau_1^2 c^2}{4} = 0 \tag{2}$$

where $-D_1 < x < 0$ and $0 < y < D_2$. Due to the multipath and wall geometry, three additional virtual sensors are present. The virtual sensors due to multipath from the side walls are located at $(+D_x,0)$ and $(+D_x - 2D_1,0)$, while the virtual sensor due to the back wall is located at $(-D_x,2D_2)$. The second TOA corresponds to a bistatic configuration involving the true and virtual sensors which form foci of a target ellipse. The equations for the three possible ellipses are given by

$$\frac{4x^2}{\tau_2^2 c^2} + \frac{4y^2}{\tau_2^2 c^2 - 4D_x^2} - 1 = 0 \tag{3}$$

$$\frac{4(x + D_x)^2}{\tau_2^2 c^2 - 4D_2^2} + \frac{4(y - D_2)^2}{\tau_2^2 c^2} - 1 = 0 \tag{4}$$

$$\frac{4(x + D_1)^2}{\tau_2^2 c^2} + \frac{4y^2}{\tau_2^2 c^2 - 4(D_1 - D_x)^2} - 1 = 0 \tag{5}$$

We hypothesize that the second arrival belongs to a multipath from any of the three surrounding walls and find the point(s) of intersection between the corresponding ellipse and the direct path circle.

In general, a circle and an ellipse can intersect at 4 possible points. However, due to the structure of the underlying problem, an ellipse corresponding to the side wall will intersect with the circle corresponding to the direct path at only one valid location, while the back wall can result in

two possible solutions. This reduces the maximum number of possible solutions to four, when considering pairs of arrivals one at a time, with the direct path being one of the two components. More specifically, when the second arrival is due to a reflection from the right side wall, the solution of (2) and (3) provides the *x*-coordinate of the possible target location as

$$x = \frac{\tau_2^2 c^2/4}{D_x}\left(\frac{\tau_1}{\tau_2} - 1\right). \quad (6)$$

Similarly, to find the *x*-coordinate of the candidate solution when the second arrival is due to a reflection from the left wall, we solve (2) with (5) to obtain

$$x = \frac{-D_1^2 + D_x D_1 + \tau_2^2 c^2/4 - \tau_1 \tau_2 c^2/4}{D_1 - D_x}. \quad (7)$$

The associated *y*-coordinates in both cases are found by substituting the values of the *x*-coordinates in (2). For the back wall case, we solve (2) with (4) and obtain the following coordinates

$$y = \frac{D_2^2 - \tau_2^2 c^2/4 + \tau_1 \tau_2 c^2/4}{D_2} \quad (8)$$

$$x = \pm\sqrt{\frac{\tau_1^2 c^2}{4} - y^2} - D_x \quad (9)$$

Note that *x* can have two values.

To maintain a candidate target location, the major and the semi-major axes of the corresponding ellipses must assume positive values. In the very special case where the target exists co-linearly between the physical sensor and the virtual sensor corresponding to the back wall, the equation of the ellipse reduces to that of a line, leading to a single solution. It can be readily shown that the conditions for a solution to exist due to multipath from the right, back, and left walls, respectively, can be expressed as $\tau_2 > \frac{2D_x}{c}$, $\tau_2 > \frac{2D_2}{c}$, and $\tau_2 > \frac{2(D_1 - D_x)}{c}$.

The number and nature of the possible solutions of target location are dependent on the radar location and the room geometry. To resolve this ambiguity, we use the directivity inherent in the UWB antenna to choose the most probable solution amongst all candidates. We reproduce the multipath scenario corresponding to each candidate solution taking into account the antenna characteristics and orientation, and compare the corresponding synthesized returns with the actual received signal. The synthesized return having the highest correlation with the actual return identifies the most probable target position.

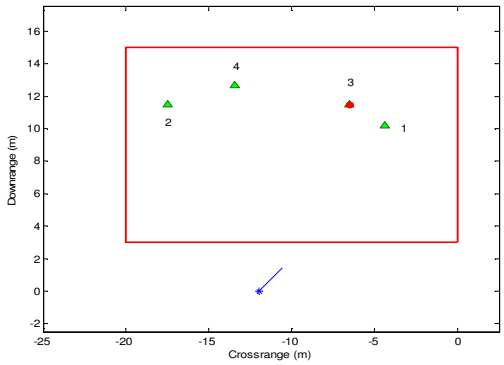

Fig. 3. Possible candidates and considered geometry with target at (-6.5, 11.5)m.

III. Simulation Results

We redesigned the EM simulator presented in [10] to not only accept the wall configuration, antenna position, and polarization as simulation parameters, but also allow for oblique incidence at the receiver. This simulator, which is based on a TEM horn antenna [11], was used to simulate the geometry in Fig. 2 with $D_1 = 15\text{m}, D_2 = 20\text{m}$, target located at (-6.5,11.5)m and the radar at (-12,0)m with the antenna oriented in the direction indicated by the red arrow. The direct reflection arrives at τ_1=84.98 ns and the TOA of the second arrival corresponding to a single-bounce multipath component is 106.83 ns. Fig. 3 illustrates the four possible candidate target positions in this case. The arrow at the sensor depicts the antenna direction. The candidate solution marked with 3 is the true target position. Fig. 4 shows the actual radar return and the simulated directional profiles for the candidate solutions 1 through 4 of Fig. 3. The knowledge of antenna characteristics and its orientation is incorporated when reproducing the candidate profiles. The highest correlation between the actual radar return and the candidate profiles resulted in the third candidate solution to be selected as the estimated target location. It is worth noting that the simulated returns corresponding to candidate solutions 2 and 4 have arrivals that occur before τ_2. If we are able to further strengthen our assumption that no multipath components are missed, then these two solutions can be dropped even before the correlation step.

IV. Sensitivity to Timing Errors

Amongst other factors, the performance of the proposed localization scheme is dependent on the accuracy of the TOA estimates of the direct and the multipath components. In this section, we quantify the impact of the TOA errors on the target location estimate.

Let $\Delta\tau_1$ and $\Delta\tau_2$ be the errors in τ_1 and τ_2, respectively. Let the estimated target location under TOA errors be $(x + \Delta x, y + \Delta y)$. Then,

$$\Delta x = \frac{\partial x}{\partial \tau_1}\Delta\tau_1 + \frac{\partial x}{\partial \tau_2}\Delta\tau_2 \quad (10)$$

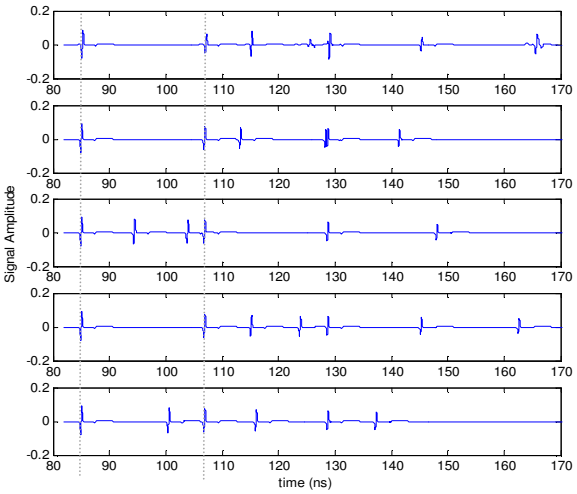

Fig. 4. Actual target return (top) and the simulated received signal for the four candidate target positions. True target at (-6.5, 11.5)m

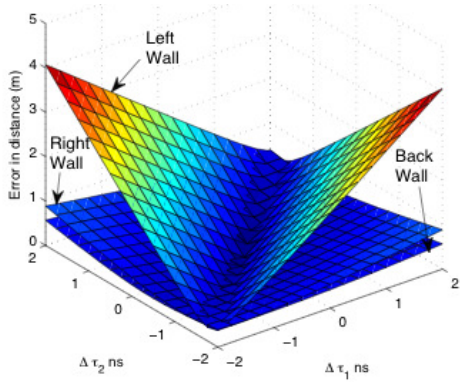

Fig. 5. Distance between the true and estimated target locations under TOA errors.

$$\Delta y = \frac{\partial y}{\partial \tau_1}\Delta\tau_1 + \frac{\partial y}{\partial \tau_2}\Delta\tau_2 \qquad (11)$$

The expressions for the various partial derivatives in (10) and (11) for the three cases of single bounce multipath are provided in Table I. For the simulation example considered in Fig. 2 where the radar is located at (-12, 0) m and the target is located at (-6.5, 11.5) m, the corresponding distance $\sqrt{\Delta x^2 + \Delta y^2}$ between the true and estimated target positions, is illustrated in Fig. 4. It is worth noting that the distance is maximum when $\Delta\tau_1$ has an opposite sign compared with $\Delta\tau_2$ for the case of multipath originating from the side walls. When the second arrival is due to the back wall, then the distance is a weak function of $\Delta\tau_2$. The third candidate corresponding to a second reflection from the left side wall resulted in the maximum sensitivity to timing error as demonstrated by Fig. 4. This is attributed to the fact that the target for the chosen geometry is much farther away from the left side wall compared to the right side and back walls, resulting in a much larger value for τ_2 in this case. This, in turn, causes the error in target location to be much larger than that for the other walls (See Table I).

Table I. Partial derivatives in (10) and (11).

Right Wall	Left Wall
$\frac{\partial x}{\partial \tau_1} = \frac{c^2}{4D_x}\tau_2$ $\frac{\partial x}{\partial \tau_2} = \frac{c^2}{4D_x}(\tau_1 - 2\tau_2)$	$\frac{\partial x}{\partial \tau_1} = \frac{-c^2}{4(D_1 - D_x)}(\tau_2)$ $\frac{\partial x}{\partial \tau_2} = \frac{-c^2}{4(D_1 - D_x)}(\tau_1 - 2\tau_2)$
$\frac{\partial y}{\partial \tau_1} = \frac{1}{2}\left(\frac{\tau_1^2 c^2}{4} - (x + D_x)^2\right)^{-\frac{1}{2}}\left(\frac{2\tau_1 c^2}{4} - 2(x + D_x)\frac{\partial x}{\partial \tau_1}\right)$ $\frac{\partial y}{\partial \tau_2} = \frac{1}{2}\left(\frac{\tau_1^2 c^2}{4} - (x + D_x)^2\right)^{-\frac{1}{2}}\left(-2(x + D_x)\frac{\partial x}{\partial \tau_2}\right)$	
Back Wall	
$\frac{\partial y}{\partial \tau_1} = \frac{c^2}{4D_2}\tau_2$ $\frac{\partial y}{\partial \tau_2} = \frac{c^2}{4D_2}(\tau_1 - 2\tau_2)$	
$\frac{\partial x}{\partial \tau_1} = \pm\frac{1}{2}\left(\frac{\tau_1^2 c^2}{4} - y^2\right)^{-\frac{1}{2}}\left(\frac{2\tau_1 c^2}{4} - 2y\frac{\partial y}{\partial \tau_1}\right)$ $\frac{\partial x}{\partial \tau_2} = \pm\frac{1}{2}\left(\frac{\tau_1^2 c^2}{4} - y^2\right)^{-\frac{1}{2}}\left(-2y\frac{\partial y}{\partial \tau_2}\right)$	

V. CONCLUSION

In this paper, we presented a new non-coherent approach for indoor target localization by exploiting multipath from surrounding walls. The proposed approach is fundamentally different from exisiting ones in that it allows solving for target position coordinates using only the direct return and one multipath return. This was made possible by using pulse shape dependency on DOA of the radar return to resolve ambiguity and for excluding false target locations. This capability becomes important when exploitation of all possible multipath returns fails due to obstruction or weak signal detection. The effectiveness of the proposed approach was shown through simulation results.

REFERENCES

[1] P. Setlur, M. Amin and F. Ahmad, "Multipath model and exploitation in through-the-wall and urban radar sensing," *IEEE Trans. Geosci. Remote Sens.*, vol. 49, no. 10, pp. 4021-4034, 2011.

[2] S. Kidera, T. Sakamoto and T. Sato, "Extended Imaging Algorithm Based on Aperture Synthesis With Double-Scattered Waves for UWB Radars," *IEEE Trans. Geosci. Remote Sens.*, vol. 49, no. 12, pp. pp.5128-5139, 2011.

[3] M. Leigsnering, F. Ahmad, M. Amin and A. Zoubir, "Multipath exploitation in through-the-wall radar imaging using sparse reconstruction," *IEEE Trans. Aerosp. Electronic Syst.*, In press.

[4] P. Setlur, G. Smith, F. Ahmad and M. Amin, "Target localization with a single sensor via multipath exploitation," *IEEE Trans. Aerosp. Electronic Syst.,* vol. 48, no. 3, pp. 1996-2014, 2012.

[5] G. Gennarelli and F. Soldovieri, "A linear inverse scattering algorithm for radar imaging in multipath environments," *IEEE Geosci. Remote Sens. Lett.,* vol. 10, no. 5, pp. 1085-1089, 2013.

[6] M. Leigsnering, F. Ahmad, M. Amin and A. Zoubir, "Compressive sensing based specular multipath exploitation for through-the-wall radar imaging," in *Proc. IEEE ICASSP*, 2013, pp. 6004-6008.

[7] Kidera, T. Sakamoto and T. Sato, "Experimental study of shadow region imaging algorithm with multiple scattered waves for UWB radars," *Progress in EM Research*, vol. 5, no. 4, pp. 393-396, 2009.

[8] G. E. Smith and B. G. Mobasseri, "Multipath exploitation for radar target classification," in *Proc. IEEE Radar conf.,* 2012, pp. 623-628.

[9] M. G. Amin, *Compressive Sensing for Urban Radar*, CRC Press, 2014.

[10] A. H. Muqaibel and U. M. Johar, "Directional UWB channel simulator," in *Proc. 6th Workshop Positioning, Navigation, Commun.,* 2009.

[11] A. Muqaibel and U. Johar, "UWB multipath simulator based on TEM horn antenna," in *Proc. 2nd Int. Conf. Wireless, Broadband, Ultra Wideband Commun.,* 2007.